Reports of Biochemistry & Molecular Biology
Vol.11, No.2, July 2022

Original article

www.RBMB.net

Regulation of Focal Adhesion Dynamics and Cell Migration by PLC/PI3K-Mediated Metabolism of PtdIns (4,5) P2 in a Breast Cancer Cell Line

Dhurgham Al-Fahad*[1], Firas Alyaseen[1], Ahmed Al-Amery[2], Clementino Ibeas Bin[3]

Abstract

Background: Focal adhesions (FAs) are highly dynamic complex structures that assembled and disassembled on an ongoing basis. The balance between the two processes mediates various aspects of cell behavior, ranging from cell adhesion to cell migration. Assembly and disassembly processes of FAs are regulated by a variety of cellular signaling proteins and adaptors. We previously demonstrated that local levels of Phosphatidylinositol 4,5-bisphosphate (PtdIns(4,5)P2) in MDA-MB-231 cells increases during FA assembly and declines during disassembly. In this study we aimed to investigate whether PtdIns(4,5)P2 regulates FA turnover.

Methods: MDA-MB-231 cells were co-transfected with a labeling vinculin (or zyxin) and the PLC**δ**1-PH biosensor to visualize FA localization and PtdIns(4,5)P2 in the cell membrane. We also used pharmacological inhibitors to determine the mechanism underlying the changes of PtdIns(4,5)P2 level during FA turnover and cell migration. Immunostaining, immunoprecipitation, and Western blotting were used to examine the localization and interaction between phospholipase C (PLC)/phosphatidylinositol 3-kinase (PI3K) FA proteins.

Results: We showed that inhibition of PLC, PI3K significantly reduced the decline of PtdIns(4,5)P2 levels within FA disassembly and the slowdown rate of FA turnover and cell migration. We also showed that the inhibition of enzymes implicated in the downstream pathway of PtdIns(4,5)P2, such as diacylglycerol kinase (DAGK) and protein kinase C (PKC) significantly reduced FA turnover time and the speed of cell migration. Additionally, we demonstrated that PLC but not PI3K interact with FAs. In conclusion,

Conclusions: This study suggests that dynamical changes of PtdIns(4,5)P2 might regulate FA turnover and facilitate cell migration.

Keywords: Cell Migration, Focal Adhesion Turnover, MDA-MB-231 Breast Cancer Cell Line, Ptdins(4,5)P2, PLC, PI3K.

Introduction

Focal adhesions (FAs) are complex structures consisting of about 150 proteins and are essential parts of the process of cell migration(1,2,3,4). FA proteins are recruited and activated by integrins, which in turn are connected to the extra cellular matrix (ECM), playing an important role in transmitting signals from inside to outside of the cell, and vice-versa (5). There are two types of FAs, called nascent and mature FAs, which participate in cancer cell migration through their assembly and disassembly processes. Nascent FAs recruit additional proteins and become larger to form mature FAs (6). Mature

1: Department of Pharmaceutical Sciences, College of Pharmacy University of Thi-Qar, Iraq.
2: Faculty of Education, Soran University, Erbil, Kurdistan Region, Iraq.
3: Ilumix Biotech Ltd, London, United Kingdom.
***Corresponding author: Dhurgham Al-Fahad; Tel: +96 47736332794; Email: dhurgham.alfahad@sci.utq.edu.iq.**
Received: 6 Jan, 2022; Accepted: 14 Jan, 2022

FAs contain adaptor and scaffold proteins, such as talin, vinculin, paxillin and zyxin, amongst others, and are approximately 1-5 µm in size (1). Collectively, these FA proteins transfer the intracellular response to the ECM, thereby communicating with the surrounding environment (5). FAs originate through interactions between talin and the β-subunit of integrin6. The head domain of talin binds with integrin, while its rod domain has several binding sites, which recruit and interact with many intracellular proteins, such as vinculin and α-actinin, to form nascent FAs (7). Extending FAs tend to advance the cell membrane, making FA assembly an important step in the forward movement of cells (7). FA disassembly can occur in association with retraction of the trailing edge of the cell during turnover, which is regulated by calpain 8 and microtubules (8). There are several factors involved in the regulation of FA assembly and disassembly, including phosphotidylinositol (PI), which forms ∼10–20% (mol%) of total cellular phospholipids, and PtdIns(4,5)P2, which forms∼0.2–1% of them (9). Despite these small quantities, PtdIns(4,5)P2 plays an important role in regulating many biological processes by recruiting additional proteins to FA sites. These include PI hydrolysis by enzymes, such as PLC, and PI kinases, such as phosphatidylinositol 3-kinase (PI3K)(10-13). These play a role in the regulation of cellular processes, by metabolizing phosphotidylinositols (11-13). Pleckstrin Homology (PH) domains contain 120 amino acids, and consist of a seven-strand β-barrel, two anti-parallel β sheets and a C-terminal α helix (14). PH domains contain β1, β2, β3 and β4 loops, which bind with the inositol ring of phosphoinositide (14). Around 10% of all PH domains have a high binding affinity for specific phosphoinositides (15,16). For example, PtdIns(4,5)P2 has a high binding affinity and specificity for PLCδ PH domains, due to neighboring phosphates in the former's inositol ring.

This binding specificity of phosphoinositides for different types of PH is important in the recruitment of a variety of kinases and enzymes to the cell membrane, allowing them to perform their function and to interact with other signaling pathways (15). In turn, some of these kinases phosphorylate the inositol ring, generating new phosphoinositides. For example, PI3K phosphorylates PtdIns(4,5)P2 to PtdIns(3,4,5)P3. Alternatively, these membrane-recruited enzymes may act on specific phosphoinositides to produce new second messengers, an important example being PLC cleaving of PtdIns(4,5)P2 to inositol trisphosphate (IP3) and diacylglycerol (DAG) (16, 18). While the changes of PtdIns(4,5)P2 level during FA assembly and disassembly has been studied, it is important to know the reasons for these dynamic changes in the level of PtdIns(4,5)P2 during FA turnover. Thus, the aim of this study is to understand the reasons for these changes in the local level of PtdIns(4,5)P2 during FA turnover in cancer cell migration.

Materials and Methods

Cell culture

MDA-MB-231 human adenocarcinoma cells were obtained from the American Type Culture Collection (ATCC, Manassas, VA). The cells were grown and maintained in Dulbecco's Modified Eagle's Medium 1x, supplemented with 10% (v/v) fetal bovine serum (FBS, Gibco) and 1% v/v Penicillin/Streptomycin (Gibco). The cells were tested routinely for mycoplasma using a Mycoplasma kit (Cat No. K1-0210, EZ-PCR Mycoplasma Test Kit, 20 assays).

Construction of the fluorescent biosensor

To generate a construct encoding the PLC**δ**1-PH-mCherry biosensor, a fragment of PLC**δ**1-PH was amplified by polymerase chain reaction (PCR) using PLC**δ**1-PH-GFP (Addgene; Plasmid #21179) as template and two primers:5'-AGCTAGATCTTTACTGGATGTTGAGC TCCT-3'(forward) and 5'-AAGTCCCGGCCCGAGTCCATGGATCC AGCT-3'(reverse). The resulting PCR product was subsequently digested with

Bgl11 and *EcoR1*, then cloned into the *Bgl11* and *EcoR1* sites of the mCherry-C1 construct (Addgene; #632524).

Inhibitors' preparation

Stocks of PLC inhibitor U73122 (TOCRIS Cat. No. 1268), U-73343 inactive analog of U73122 (TOCRIS Cat. No. 4133), PI3K inhibitors LY294002 (TOCRIS Cat. No. 1130), LY 303511 inactive analog of LY294002 (TOCRIS Cat. No. 2418), DAG inhibitor R59-022 (TOCRIS Cat. No. 2194) and PKC inhibitor Go6976, (TOCRIS Cat. No. 2253) were prepared by dissolving them in DMSO according to their product information sheet instruction. These inhibitors were aliquoted into labeled sterile eppendorf tubes in a culture hood, then stored at -20 °C.

Co-transfection assay and live imaging

The amount of 4.41 mg/ml chilled rat tail type I collagen (BD Bioscience) was used for coating ibidi glass bottom dishes. Then, the dishes were seeded with 1 x 105 MDA-MB-231 cells until 70% confluence. 3 µg vinculin/zyxin GFP and PLC**δ**1-PH-mCherry were added in 100 µl of serum-free media. Then, 6 µl of polyethylenimine (PEI) transfection reagent was added into the tubes and was gently stirred. The tubes were incubated for 15 minutes in the culture hood. Then the mixture of GFP and mCherry-PH/PEI was placed into the ibidi dish containing 2 ml of complete media and incubated overnight under cell culture conditions. The ibidi dish was placed into the confocal chamber and coupled to CO2 supply and warmed at 37 °C initially for 30 minutes. mCherry (568 nm) and GFP (488 nm) were used to visualize the co-localization between PtdIns(4,5)P2 and vinculin/zyxin-containing FAs. To quantify the PtdIns(4,5)P2 decline within FA disassembly, confocal live images were taken using the same objectives 40x and laser settings (Nikon Eclipse Ti Laser-scanner). ImageJ (RRID:SCR_003070) was used to measure the level of PtdIns(4,5)P2 and FA turnover. The region of interest (ROI) was firstly selected closely around FAs, then this ROI was applied to the mCherry-channel of PtdIns(4,5)P2 to determine the specific localisation of PtdIns(4,5)P2 within FA disassembly. The whole cycle of FA turnover was observed. The FA was absent both in the beginning and at the end of the time-lapse series. The intensity of PtdIns(4,5)P2 was measured from the same time frame that the FAs was measured until the last frame in which FAs disassembly finished.

Live-cell time-lapse microscopy

After coating a 6 well-plate with fibronectin (20 µg/ml), the plate was seeded with MDA-MB-231 cells. The next day, new media was used with of PLC U73122, PI3K LY294002, DAG R59-022 (3 µM) or PKC Go 6976 (10-3µM) inhibitors. U-73343 (0.5 µM) and LY 303511 (25 µM) were used as a control for each inhibitor. The old media was removed, and 2 ml of new media was added in each well of the plate with an appropriate concentration of the inhibitor. The plate was sealed with parafilm, and a hole was made at the edge of plate to insert the CO2 supply needle. The heater was set at 37 °C, 2 hours before time-lapse. The plate was placed on the stage of the Nikon Tie time-lapse microscope and a 10x objective was used for image acquisition images. Images were takenat 15-minutes interval for 24 hours. The camera was chosen as live-fast to capture live images with normal high quality. X/Y positions were selected which enabled free movements between the selected points. Perfect focus system (PFS) was used to reduce axial focus change during long-time imaging. E100 was changed to L100, then 5 positions were taken for each well. ImageJ was used to analyze the speed of cell migration in non-treated and treated cells. 30 cells of each well were measured using the equation: Speed of cell= Total length of cell (µm) / time.

Immunocytochemistry

After transfection of MDA-MB-231 cells with PLC**δ**1-PH-GFP/mCherry, the media was aspirated and washed with pre-warmed PBS

once. Then, one ml of 4% PFA was added to each well for 20 minutes to fix cells at room temperature. 1ml of PBS was added for washing (three times each wash 10 minutes). One ml of 0.5 % Triton-X 100 was added for permeabilization of cells for 10 minutes at room temperature. The cells were then washed with PBS three times (each wash 10 minutes). One ml of 10 % goat serum was added around 30 minutes for blocking. The cells were incubated with rabbit anti-vinculin (Abcam; ab130007) orrabbit anti-zyxin (supplied by Prof Phil Dash, University of Reading) antibodies and with mouse anti-PLC (or mouse anti-PI3K). Bothmouse anti-PLC and PI3K antibodies were supplied by Prof Phil Dash (University of Reading). All primary antibodies diluted in 1:10 in PBS supplemented with 2% goat serum were incubated with the cells for 1 hour. The cells were washed three times with PBS for 10 minutes each time then were incubated with 488 Alexa Fluor anti-mouse (Cell Signalling; 4408) at a dilution of 1:10 for 1 hour. The cells were washed with PBS three times for 10 minutes each time and were stained with DAPI (4',6-diamidino-2-phenylindoleisa fluorescent stain that interacts with DNA which mix with fluoroshield Mounting Medium) on the glass slide. Nail polish was used to attach the coverslips onto the slides.

Immunoprecipitation (IP) and Western blotting (WB)

Four hundredµl of the lysate was incubated with primary antibody using mouse anti-PLC and PI3K antibodies. Then, the tube was rotated at 4 °C overnight to precipitate PLC and PI3K. Protein A/G agarose beads (Santa Cruz, USA) were prepared according to the manufacturer's instructions. Then, the collected supernatant was used for WB to detect the interaction of vinculin and zyxin. The membrane was incubated overnight in the cold room with primary antibody rabbit anti-vinculin and anti-zyxin (1: 1000) in 2% bovine serum albumin (BSA). The next day, the membrane was washed three times with 1x TBST (Sigma Aldrich), each was washed 10 minutes. HRP secondary antibodies (Cell Signalling; 7076 and 7074) were added 1:2000 in 2% BSA to the membrane and shook for 1 hour. Then, the membrane was washed with 1xTBST, each was washed 10 minutes. 2 ml of ECL prime detection (1 ml of the solution and 1 ml of solution B) was used and incubated for 1 minute in the dark. The bands were detected by Image Quant LAS 4000 minim (GE Healthcare). Rabbit IgG antibody was used as a negative control.

Statistical analysis

One-way analysis of variance after Dunn's multiple comparisons was used for statistical analysis. GraphPad Prism 5 software (GraphPad Software, San Diego, CA) was used for statistical comparisons. Three independent experiments in triplicate (n= 3) and p values< 0.05 were considered statistically significant.

Results

Quantification of PtdIns(4,5)P2 level during FA turnover

MDA-MB-231 cells, an epithelial, human breast cancer cell line, were transfected with PLCδ1-PH-GFP. The cells were fixed with paraformaldehyde and immunostained for anti-vinculin antibody and then stained with Alexa Fluor secondary antibody to visualise the spatial interaction between PtdIns(4,5)P2 and vinculin (Fig.1A). The Z-Stacking-single slice was performed through taking different slices to record the entire cell membrane from the bottom to the top. Then, single slice was selected to determine an accurate co-localization point between a single vinculin and PtdIns(4,5)P2. Spatial co-localization was measured between PtdIns(4,5)P2 and vinculin. Our results showed that Spearman's rank correlation value values were moderate. Cells treated with the PLC inhibitor U73122 (0.5 µM) or the PI3K inhibitor LY294002 (25 µM) inhibitors exhibited greater correlation between the localization of PtdIns(4,5)P2 and vinculin the localization PtdIns(4,5)P2 and vinculin compared their corresponding control analoguesU-73343 (0.5 µM) and LY

303511 (25 μM), respectively. Our results showed that the co-localization value was increased from 0.37±0.02 to 0.50±0.05, with U73122 and to 0.43±0.03, LY294002 (Fig. 1B). Later, co-transfection was performed to investigate spatiotemporal organization of PtdIns(4,5)P2 within FA turnover using biosensor (PLC**δ**1-PH) specific for PtdIns(4,5)P2 and GFP- vinculin/zyxin for FA localization in breast cancer cell line MDA-MB-231. Later, the cells were co-transfected with mCherry/RFP-vector (used as a control) or PLC**δ**1-PH-mcherry with GFP/RFP vinculin/zyxin. Our result also showed that mCherry/GFP-vector was at a constant level during FA assembly and disassembly (Fig. 2A), and PLC**δ**1-PH-mcherry levels increased during FA assembly, then declined during FA disassembly (Figs. 2B and 2C).

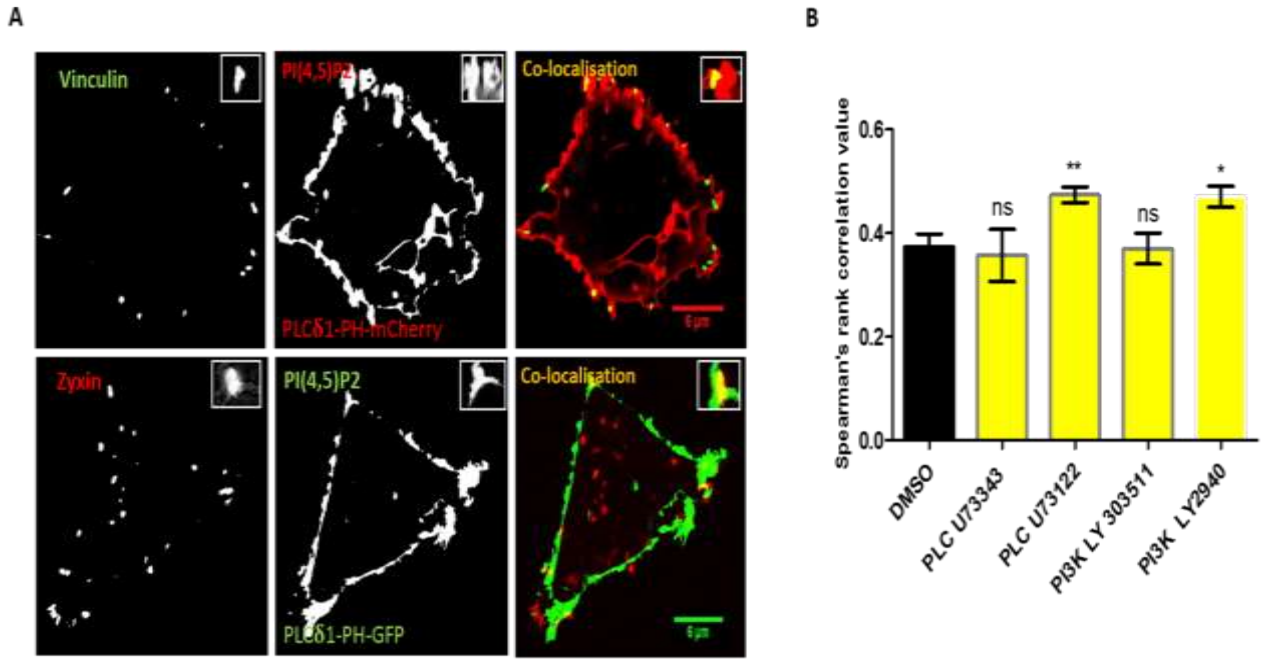

Fig. 1. Spatial co-localisation between PtdIns(4,5)P2and a single FA in MDA-MB-231 cells on. **A**) MDA-MB-231 cells were transfected with PLC**δ**1-PH-mCherry and immunostained for vinculin (green) to visualise the spatial interaction between PtdIns(4,5)P2and FAs. The highlighted areas show a magnification of the spatial co-localization region between PtdIns(4,5)P2 and a single FA. Spearman's (rho) correlation coefficient analysis was used to measure co-localization value between ROI of PtdIns(4,5)P2 and vinculin. The co-localization values between vinculin and PtdIns(4,5)P2 were shown to be moderate. Three independent experiments were performed, but only representative pictures are shown. Scale bars= 6 μm. **B**) Cells were treated with PLC inhibitor U73122 (0.5 μM) and PI3K inhibitor LY294002 (25 μM) for 30 minutes, the co-localization value between PtdIns(4,5)P2 and vinculin was increased compare with control. Statistical analysis was performed by One-way ANOVA with Dunnett's Multiple Comparison Test. Statistical significance differences were accepted at **p≤ 0.005. Data are a representative of the means±SD of three independent experiments in which n= 20 cells were measured, and the number of a single FA measured per cell was 40.

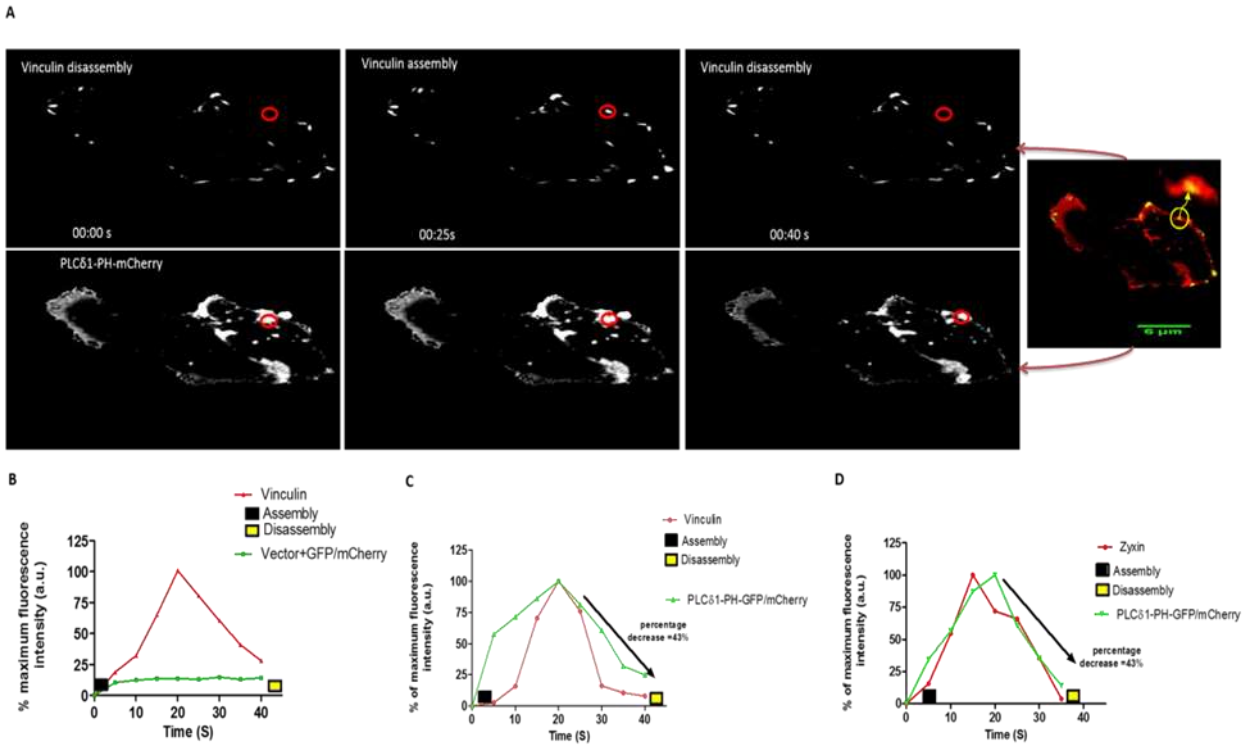

Fig.2. Quantification of local levels of PtdIns(4,5)P2 within areas of FAs turnover. Confocal live imaging showing local levels of PtdIns(4,5)P2 within vinculin/zyxin turnover areas over time. The MDA-MB-231 cells were co-transfected with PLC**δ**1-PH-mCherry/vector+mCherry (used as a control) and GFP-vinculin/zyxin. Z-stacks were taken at 0.15 µm distance with time-lapse series acquired over a 10-minute period with an interval of 15 seconds. The first row refers to assembly and disassembly of FAs, while the second row refers to local levels of PtdIns(4,5)P2 within FAs turnover areas. **A**) The highlighted areas show the region of interest that was drawn closely around the FAs and the PtdIns(4,5)P2, and used to measure the specific localization of local levels of PtdIns(4,5)P2 within FAs. The FA selected for measuring should be absent both in the beginning and the end of the time-lapse series. **B**) The Quantification of dynamic change of local levels of vector+mCherry during FA assembly and disassembly. The cells were co-transfected with vector+mCherry and vinculin/zyxin. The red curve refers to the intensity measurement of vinculin/zyxin assembly and disassembly over a time course (40 seconds). The green curve refers to the intensity measurement ofvector+mCherry which was at a constant level during vinculin/zyxin assembly and disassembly over a time course (40 seconds). **C, D**) The Quantification of dynamic change of local levels of PLC**δ**1-PH-mCherry during FA assembly and disassembly. The cells were co-transfected with PLC**δ**1-PH-mCherry and vinculin/zyxin. The red curve refers to the intensity measurement of vinculin/zyxin assembly and disassembly over a time course (40 seconds). The green curve refers to the intensity measurement of local increased and declined of PtdIns(4,5)P2 levels within talin/paxillin assembly and disassembly over a time course of 40 seconds.

Inhibition of PLC and PI3K signaling reduced the decline of PtdIns(4,5)P2 levels during FA disassembly

In order to determine whether the cause of the decline of PtdIns(4,5)P2 during FA disassembly was related to PLC and PI3K signaling, we inhibited PLC and PI3K for 30 min. Our results showed that the percentage decline of PtdIns(4,5)P2 during FA disassembly was significantly reduced after the treatment of the PLC and PI3K inhibitors from 41.0±1.0% to 5.0±1.1%, and to 34.0±0.6% respectively (Fig. 3). At the same time, both inhibitors were shown to significantly increase the duration of FA turnover, since it increased from 32±0.6 s to 43±0.9 s(U73122) and 39±0.9 s(LY294002). The speed of cell migration was found to be reduced with PLC and PI3K inhibition, as it was shown to change from 13.7±0.9 µm/h to 8.3±0.4 µm/h and 10±0.6 µm/h (Fig. 4).

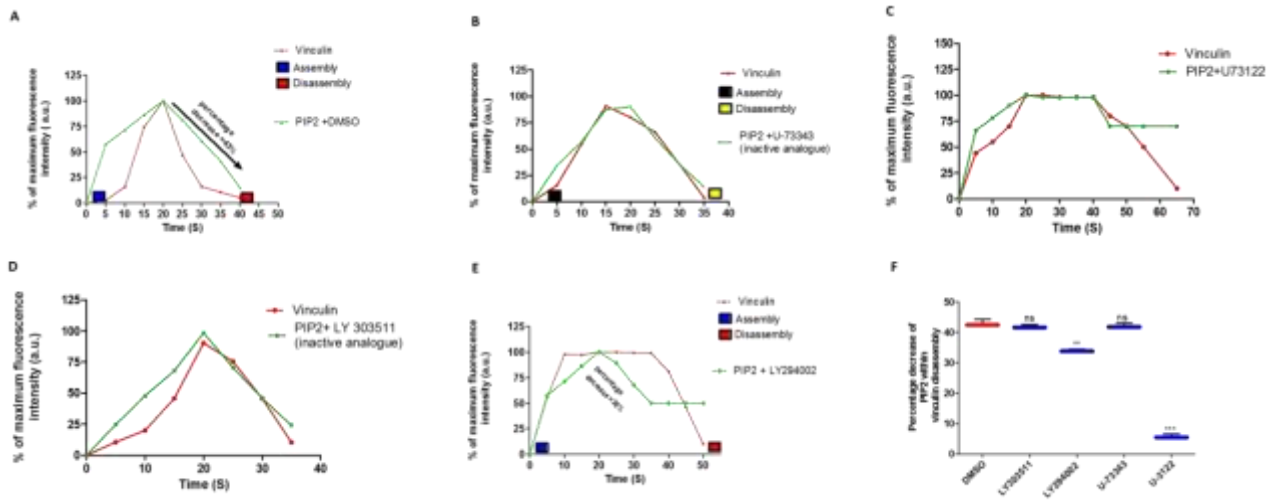

Fig. 3. PLC and PI3K pathway knockdown reduced the decline of PtdIns(4,5)P2 during FA disassembly and slow down the rate of FA turnover**. A-F)** The decline of PtdIns(4,5)P2 was significantly reduced by PLC and PI3K inhibitors for 30 minutes, comparedthe PLC U-73343 and LY 303511 inactive analogues that was used as a control at the same dose and time. This data was resulted from 40 representative FA intensity profiles per cell. Statistical analysis was performed by one-way ANOVA with Dunnett's test for multiple comparison. Statistical significance was accepted at *** p< 0.0005. Data represents mean±SD of the three independent experiments.

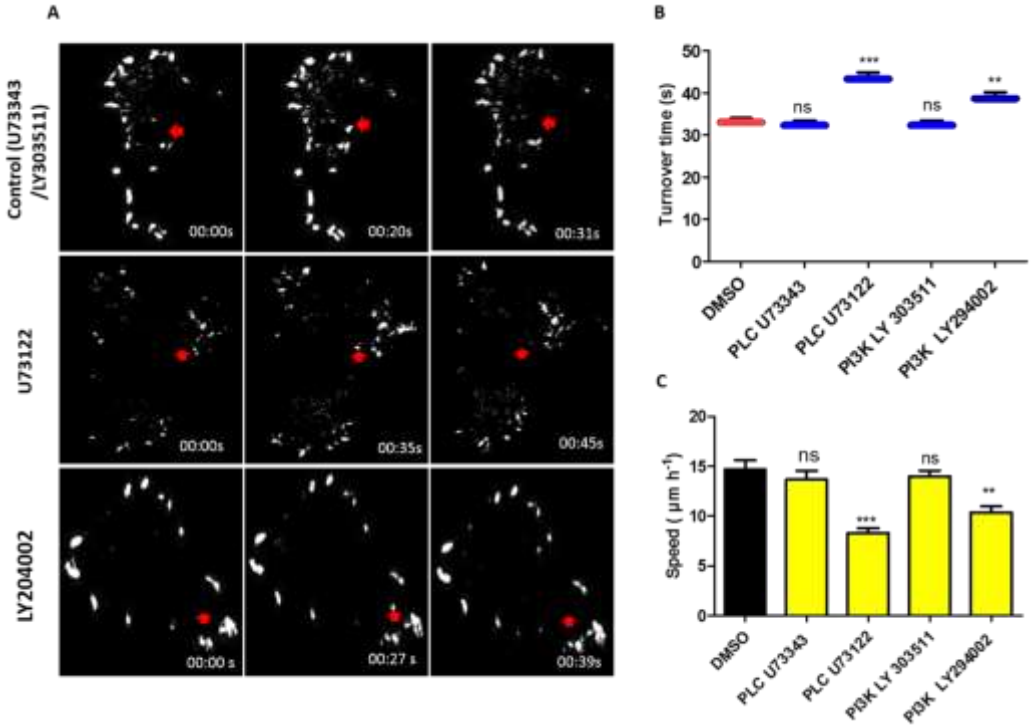

Fig. 4. Inhibiting PLC, PI3K pathway reduced FA disassembly time of MDA-MB231cells. **A**) Confocal live imaging showing vinculin turnover over time. The red arrow shows dynamic FAs. MDA-MB-231 cells were transfected with GFP-vinculin for 24 h, then treated with U73122 and LY204002 inhibitors and incubated for 30 min. Treatment with U73343/LY303511 were used as a control. **B**) Statistical analysis of FA turnover rates was determined from 40 FAs, in 20 migrating MDA-MB-231. Cells treated with the inhibitors showed that FA disassembly rate was decreased significantly. **C**) Cell migration was significantly inhibited, compared to cells treated with the negative controls' analogues. Time-lapse microscopy was used to track cell migration for 24 hours. MTrackJ was used to measure cell migration. Statistical analysis was performed using one-way ANOVA with Dunnett's test for multiple comparison. Statistical significance was accepted at ***p< 0.0005. Data represents mean±SD of the three independent experiments.

DAG kinase and PKC inhibitors slowed the rate of FA turnover and the speed of cell migration

In order to examine the effect of the inhibition of further downstream pathways of PtdIns(4,5)P2 on cell migration and FA turnover, experiments were performed using the DAG kinase inhibitor R59-022 (3 μM) and the PKC kinase inhibitor Go 6976 (10-3 μM). Our results howed that both the DAG kinase and PKC inhibition significantly increase the duration of FA, from 33.0±0.6 s to 38.0±0.6 s and 39.0±0.9 s, respectively (Fig. 5). The speed of cell migration was shown to reduce with both inhibitor from 14±0.9 μm/h to 8.0±0.6 μm/h (R59-022) and 7±0.6 μm/h (Go 6976) (Fig. 5).

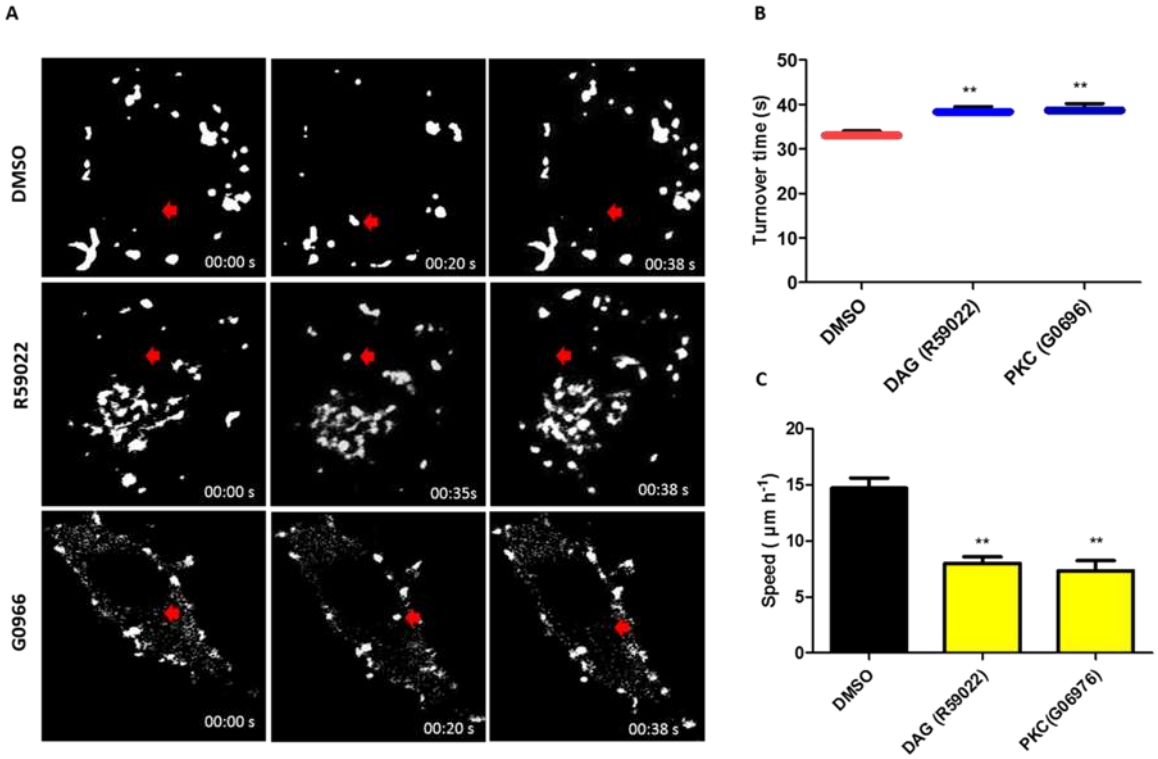

Fig. 5. Inhibiting the DAG and PKC pathways reduced FA disassembly time of MDA-MB231 cells. **A**) Confocal live imaging showing vinculin turnover over time. The red arrow shows dynamic FAs. MDA-MB-231 cells were and transfected with GFP-vinculin. 24 h post-transfection these cells were treated with R59022 and Go966 inhibitors and incubated for 30 min and treatment with DMSO 1% were used as a control. **B**) Statistical analysis of FA turnover rates was determined from 40 FAs, in 20 migrating MDA-MB-231. Cells treated with the inhibitors showed that FA disassembly rate was decreased significantly. **C**) MDA-MB-231 cell migration was significantly inhibited, compared to cells treated with the control analogues. Time-lapse microscopy was used to track cell migration for 24 h. MTrackJ was used to measure cell migration. Statistical analysis was performed by one-way ANOVA with Dunnett's test for multiple comparison. Statistical significance was accepted at ***p< 0.0005. Data represents mean±SD of the three independent experiments.

Interaction of PLC and PI3K with FAs

Next, we investigated the possible interaction between PLC/PI3K and a FA protein. Cells co-stained for PLC (red) and vinculin (green) showed from co-localization analysis that PLC's localization moderately correlated with the localization of vinculin (0.58±0.10). The results also showed that the localization of PI3K does not correlate with that of vinculin (-0.25±0.28) (Fig. 6A). To further investigate this result, we performed an immunoprecipitation assay to assess potential interactions between PLC and vinculin/zyxin and between PI3K and vinculin/zyxin. Our data showed that PLC was bound with vinculin and zyxin, whereas PI3K was bound to neither of these two FA proteins (Figs. 6B and 6C).

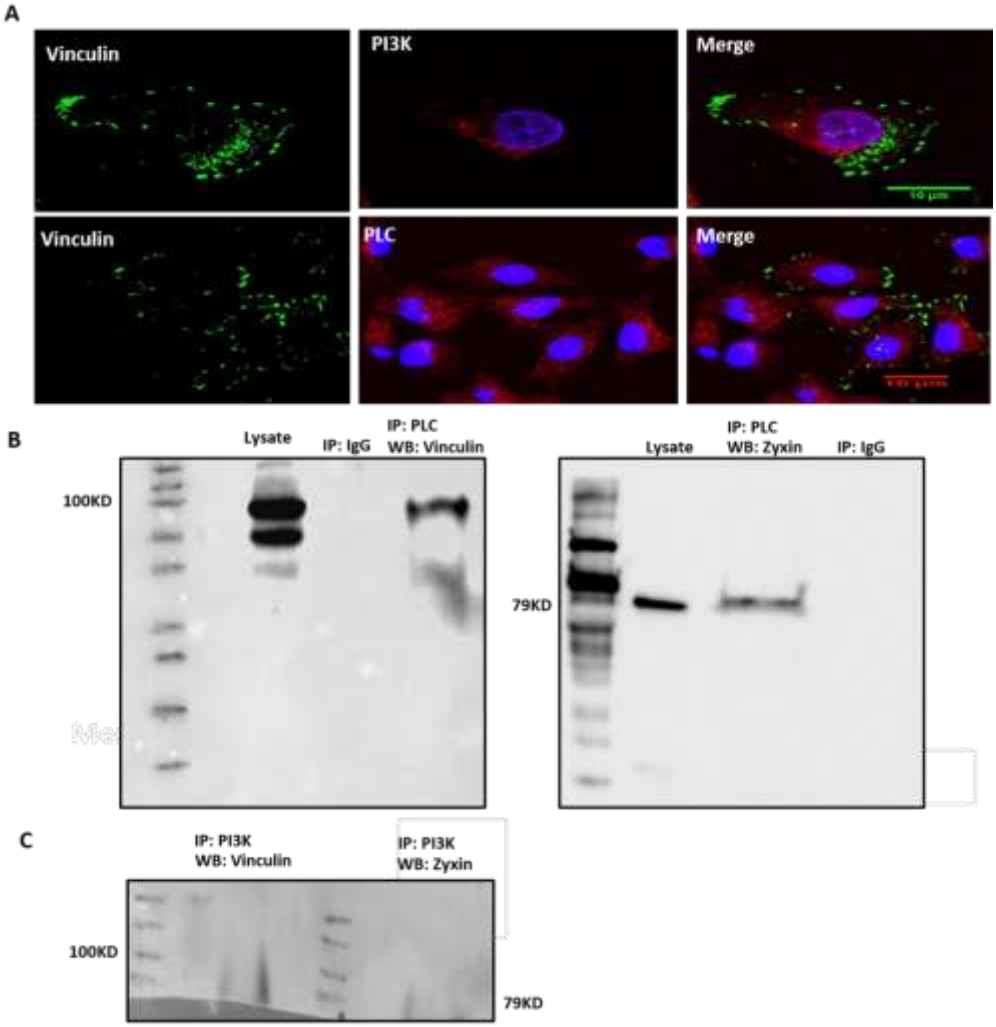

Fig. 6. A) Spatial co-localisation between PLC/ PI3K and vinculin. (A)MDA-MB-231 cells were fixed and co-stain with anti-PI3K/anti-PLC (red) and vinculin (green) antibodies, as well as with DAPI (Blue) to visualise the spatial interaction between vinculin and PI3K and between vinculin and PLC. Z-Stacking was taken with confocal microscopy. The highlighted areas are shown the magnification of spatial co-localisation region between vinculin and PI3K or PLC and found that the co-localisation value between PLC and vinculin them was 0.58±0.10 and PI3K was not co-localised with vinculin. These experiments were performed four times independently. **B**, **C**) Co-immunoprecipitates of PLC/PI3K and FAs. Proteins were extracted from MDA-MB-231 cells then incubated overnight with primary anti-PLC and PI3K antibodies. PLC and PI3K were precipitated from lysate using rabbit anti-PLC and anti-PI3K antibodies and detected by western blotting using mouse anti-PLC and anti-PI3K antibodies and mouse anti-vinculin and anti-zyxin antibodies. The results show that PLC was bound with vinculin and zyxin while PI3K was not bound with vinculin and zyxin. Rabbit IgG was used as negative control.

Discussion

Previous studies have shown that inositol phospholipid signaling is commonly seen in breast cancer, suggesting an important role for inositol lipids in cancer cell invasion (18). However, little attention has been given to study the dynamic change of PtdIns(4,5)P2 during FA turnover in order to determine the causes of changes of PtdIns(4,5)P2 levels within FA assembly and disassembly in breast cancer cells. In this study, we used the biosensor PLC**δ**-PH-GFP, which has a high binding affinity and selectivity for PtdIns(4,5)P2, and is considered to be a good probe to determine the subcellular localization of PtdIns(4,5)P2 (19). We reported that PtdIns(4,5)P2 co-localized with vinculin, with moderate correlation between the localization of both proteins(Fig. 1A). The correlation

between the localization of PtdIns(4,5)P2 and that of vinculin was found to be increased in cells treated with the PLC inhibitors(Fig. 1B). Our results demonstrated that local levels of PtdIns(4,5)P2 increased and declined concomitantly with vinculin/zyxin assembly and disassembly, respectively (Fig. 2). Monitoring the dynamic of PtdIns(4,5)P2 using a mCherry/GFP-tagged PH domain is a widely used but it raises the question of whether binding of the probe might affect the normal binding of PtdIns(4,5)P2 to its endogenous partners (including vinculin and zyxin) and therefore alter the normal FA assembly/disassembly. As a result, we used GFP/mCherry vector as a control to investigate whether there is similar dynamic of vinculin/zyxin in cells transfected with GFP/mCherry vector (Fig. 2A) and cells transfected with the GFP-PH PLC**δ**1(Fig. 2B and 2C). Our results also demonstrated that PtdIns(4,5)P2 level during FA disassembly is reduced when cells were treated with a PLC and PLC inhibitors (Fig. 3). Here we showed that altering levels of PtdIns(4,5)P2 during FA with PLC and PI3K inhibitors also affect that rate of FA turnover. Thus, suggesting that both the PLC and PI3K pathways may be implicated in the regulation of FA dynamics. Additionally, using a pharmacological approach, we showed that both the DAG kinase and PKC pathways, which are both downstream to PtdIns(4,5)P2, also regulate FA turnover and cell migration. This might suggest that FA regulations is either dependent on PtdIns(4,5)P2 or the downstream effectors of the latter, such as IP3 or DAG.

FA disassembly may occur due to hydrolysis of PtdIns(4,5)P2 by PLC, its phosphorylation by PI3K, or by the dissociation of PtdIns(4,5)P2-generating PIP5Kγ. Conversely, FA disassembly could be caused by a decline in PtdIns(4,5)P2 levels (16, 17, 20). FA disassembly might also be directly driven by DAG and IP3, which play crucial role in the activation of PKC and IP3-bound IP3Rs release of Ca2+, which in turn activates calpains, Pyk2, PKC and Ca2+/calmodulin dependent protein kinase (CaMK-II)(21-26). These effectors may trigger and cleave the nearby FA proteins that have not been disassembled by the decline of PtdIns(4,5)P2 levels (23). This possibly confirms that PLC allows disassembly of FA, either directly through hydrolysis-mediated by the reduction of local levels of PtdIns(4,5)P2, or indirectly through its downstream signaling pathways, which target FA locally. Given that PLC can directly interacts with FA, it is possible that during this interaction, PLC causes FA disassembly, either through phosphorylation/hydrolysis of PtdIns(4,5)P2 or via downstream signaling pathways. It is not clear however how would PI3K modulate the composition of FA via the modulation of local PtdIns(4,5)P2 levels. It is possible that PI3K might regulate FA dynamics by altering the total plasma membrane composition of PtdIns(4,5)P2 and its effectors. It is possible that, Vinculin/zyxin-GFP was used as a marker for FA localization and was found to be representative of FA proteins in our experimental design. This study would clearly benefit from additional experiments, such as using the binding-deficient mutant versions of the probe which can be used as a negative control, such as PLC**δ**-GFP PH domain mutant (R40L), which is a negative control of PLC**δ**-PH domain (wild type) (19). R40L mutation blocks the cytosolic translocation of PLC**δ**-PH domain (wild type), even if PLC**δ** is activated. Mutant domains that are unable to bind with phosphoinositides (19) could be used to determine the specificity of the biosensors, and to ensure that any changes that are observed in PtdIns(4,5)P2 are not a consequence of changes in the shape or amount of membrane within and around a single FA turnover (19, 27).

In conclusion, this study suggests that changes of PtdIns(4,5)P2 level during FA turnover may not be an epiphenomenon but may actually contribute to the regulation of FA assembly and disassembly, thus facilitating the migration of breast cancer cells.

Acknowledgements

The authors would like to thank the Iraqi ministry of higher education and scientific research and University of Thi-Qar.

References

1. Kanchanawong P, Shtengel G, Pasapera AM, Ramko EB, Davidson MW, Hess HF, *et al*. Nanoscale architecture of integrin-based cell adhesions. Nature. 2010;468(7323):580-4.
2. Alharbi BF, Al-Fahad D, Dash PR. Roles of Endocytic Processes and Early Endosomes on Focal Adhesion Dynamics in MDA-MB-231 Cells 31 Cells. Rep Biochem Mol Biol. 2021;10(2):145-155.
3. Al-Fahad D, Alharbi BF, Bih CI, Dash PR. Nitric oxide may regulate focal adhesion turnover and cell migration in MDA-MB-231 breast cancer cells by modulating early endosome trafficking. Med J Cell Biol. 2021;9(2):60-72.
4. Al-Fahad D. Regulation of Focal Adhesions by PtdIns(4,5)P2 and PtdIns(3,4,5)P3 in Cancer Cell Migration. University of Reading. 2018;27.
5. Wu C. Focal Adhesion: A Focal Point in Current Cell Biology and Molecular Medicine. Cell Adh Migr. 2007;1(1):13-8.
6. Nagano M, Hoshino D, Koshikawa N, Akizawa O, Seiki M. Turnover of focal adhesions and cancer cell migration. Int J Cell Biol. 2012;2012:310616.
7. Nayal A, Webb DJ, Horwitz AF. Talin: an emerging focal point of adhesion dynamics. CurrOpin Cell Biol. 2004;16(1):94-8.
8. Zaidel-Bar R, Cohen M, Addadi L, Geiger B. Hierarchical assembly of cell–matrix adhesion complexes. Biochem Soc Trans. 2004;32(Pt3):416-20.
9. Jiang G, Giannone G, Critchley DR, Fukumoto E, Sheetz MP. Two-piconewton slip bond between fibronectin and the cytoskeleton depends on talin. Nature. 2003;424(6946):334-7.
10. Giannone G, Mège R-M, Thoumine O. Multi-level molecular clutches in motile cell processes. Trends Cell Biol. 2009;19(9):475-86.
11. Balla T. Phosphoinositides: Tiny Lipids With Giant Impact on Cell Regulation. Physiol Rev. 2013;93(3):1019-1137.
12. Fogh BS, Multhaupt HAB, Couchman JR. Protein Kinase C, Focal Adhesions and the Regulation of Cell Migration. J Histochem Cytochem. 2014;62(3):172-84.
13. Chen YF, Chen YT, Chiu WT, Shen MR. Remodeling of calcium signaling in tumor progression. J Biomed Sci. 2013;20(1):23.
14. Al-Fahad, D. The possible role of PtdIns (4,5) P2 and PtdIns (3,4,5) P3 at the leading and trailing edges of the breast cancer cell line. Iberoamerican Journal of Medicine. 2021;3(1):26-32.
15.Alfahad D, Alharethi S, Alharbi B, MawloodK, Dash P. PtdIns(4,5)P2 and PtdIns(3,4,5)P3 dynamics during focal adhesions assembly and disassembly in a cancer cell line. Turk J Biol. 2020;44(6):381-392.
16. Wang X, Hills LB, Huang YH. Lipid and Protein Co-Regulation of PI3K Effectors Akt and Itk in Lymphocytes. Front Immunol. 2015;6:117.
17. A Comparative Study to Visualize Ptdins (4,5) P2 and Ptdins (3,4,5) P3 in MDA-MB-231 Breast Cancer Cell Line. Rep Biochem Mol Biol. 2022;10(4):518–526.
18. Lemmon MA. Pleckstrin Homology (PH) domains and phosphoinositides. Biochem Soc Symp. 2007;(74):81-93.
19. Izard T, Brown DT. Mechanisms and Functions of Vinculin Interactions with Phospholipids at Cell Adhesion Sites. J Biol Chem. 2016;291(6):2548–2555.
20. van den Bout I, Divecha N. PIP5K-driven PtdIns(4,5)P2 synthesis: regulation and cellular functions. J Cell Sci. 2009;122(Pt 21):3837-50.
21. Baenke F, Peck B, Miess H, Schulze A. Hooked on fat: the role of lipid synthesis in cancer metabolism and tumour development. Dis Model Mech. 2013;6(6):1353-63.
22. Várnai P, Balla T. Visualization of Phosphoinositides That Bind Pleckstrin Homology Domains: Calcium- and Agonist-induced Dynamic Changes and Relationship to Myo-[³H]inositol-labeled Phosphoinositide Pools. J Cell Biol. 1998;143(2):501-10.
23. Raucher D, Stauffer T, Chen W, Shen K, Guo S, York J D, et al. Phosphatidylinositol 4,5-bisphosphate functions as a second messenger that regulates cytoskeleton-plasma membrane adhesion. Cell. 2000;100(2):221-8.

24. Valeyev NV, Downing AK, Skorinkin AI, Campbell ID, Kotov NV. A calcium dependent de-adhesion mechanism regulates the direction and rate of cell migration: a mathematical model. In Silico Biol. 2006;6(6):545-72.
25. Easley CA, Brown CM, Horwitz AF, Tombes RM. CaMK-II Promotes Focal Adhesion Turnover and Cell Motility by Inducing Tyrosine Dephosphorylation of FAK and Paxillin. Cell Motil Cytoskeleton. 2008;65(8):662-674.
26. Tsai FC, Kuo GH, Chang SW, Tsai PJ. Ca2+ signaling in cytoskeletal reorganization, cell migration, and cancer metastasis. Biomed Res Int. 2015;2015:409245.
27. Balla T, Várnai P. Visualization of Cellular Phosphoinositide Pools with GFP-Fused Protein-Domains. Curr Protoc Cell Biol. 2009;Chapter 24:Unit 24.4.